

Finite Element Refinements for Inverse Electrocardiography: Hybrid-Shaped Elements and High-Order Element Truncation

Dafang Wang, Robert M. Kirby and Chris R. Johnson

Abstract— We study how finite element discretizations can be selected to achieve optimal numerical approximation of the inverse electrocardiographic (ECG) problem. Due to its ill-posed nature, the inverse ECG problem poses a different discretization requirement from its corresponding forward problem counterpart. Conventional refinement strategies effective for the forward problem may become ineffective when applied to the inverse problem. We propose refinement strategies specifically tackling the ill-posedness of the inverse problem. The strategies lead to two numerical methods. One is hybrid-shaped finite elements, involving quadrilateral/triangular elements in 2D and prismatic/tetrahedral elements in 3D. Another method uses high-order finite elements, extracts from the resulting system the linear component, and solves the linear part only. The hybrid element method was conducted on a realistic 3D torso model whereas the high-order truncation method was tested on a 2D segmented torso slice. Results demonstrate that both methods improve both the discrete problem’s conditioning and the inverse solution, indicating our strategies might provide guidelines for 3D mesh generation from segmented images in practical biomedical simulations.

Index Terms— electrocardiography; inverse problem; high-order finite element method; refinement

I. INTRODUCTION

The inverse electrocardiographic (ECG) problem of recovering epicardial potentials from body-surface measurements has wide applications from noninvasive diagnosis of cardiac diseases (*e.g.* ischemia) to guidance of intervention (*e.g.* ablation and defibrillation). ECG simulations include mathematical modeling of the biophysical process and geometric approximation of the anatomical structure of human bodies. We consider a model that characterizes the cardiac source by epicardial potential distribution, given as follows:

$$\nabla \cdot (\sigma(\mathbf{x})\nabla u(\mathbf{x})) = 0, \quad \mathbf{x} \in \Omega \quad (1)$$

$$u(\mathbf{x}) = u_0(\mathbf{x}), \quad \mathbf{x} \in \Gamma_H \quad (2)$$

$$\vec{n} \cdot \sigma(\mathbf{x})\nabla u(\mathbf{x}) = 0, \quad \mathbf{x} \in \Gamma_T, \quad (3)$$

$$u(\mathbf{x}) = g(\mathbf{x}), \quad \mathbf{x} \in \Gamma_T, \quad (4)$$

where Ω denotes the torso volume bounded by the epicardium Γ_H and the torso surface Γ_T . $u(\mathbf{x})$ is the potential field on Ω , u_0 is the epicardial potential, and g represents the measured body-surface potential. $\sigma(\mathbf{x})$ is a symmetric, positive-definite conductivity tensor, and \vec{n} denotes the outward facing vector normal to Γ_T . The forward problem seeks the potential field $u(\mathbf{x})$ given the cardiac source

u_0 . The inverse problem attempts to recover u_0 from the measurement g .

The governing equations are typically discretized with the finite element methods (FEM) or boundary element methods (BEM), both of which improve numerical accuracy by various refinement strategies. This paper studies discretization strategies when the FEM is used. While most refinement methods are able to achieve satisfactory accuracy for a forward problem, the ill-posedness of an inverse problem requires different refinement considerations than its corresponding forward problem [1].

The ill-posedness usually leads to an ill-conditioned numerical system. Conventional approaches for obtaining a stable solution involves imposing additional constraints, a technique called regularization. We show that the conditioning property is subject to how the FEM is applied and refined; therefore discretization itself forms one type of regularization. We propose two methods that specifically tackle the concerns of the inverse problem: (1) hybrid finite elements and (2) linear component truncation from high-order elements. Both methods alleviate the ill-conditioning of the resulting numerical system to be solved, and both can be combined with other classical regularization methods to further improve the inverse solution accuracy.

II. FEM, HYBRID ELEMENTS AND LINEAR TRUNCATION

A. Finite Element Discretization

In a theoretical FEM approach, the potential field $u(\mathbf{x})$ can be decomposed into $u(\mathbf{x}) = v(\mathbf{x}) + w(\mathbf{x})$ where $w(\mathbf{x})$ satisfies boundary conditions (2) and (3) and $v(\mathbf{x})$ is a homogeneous term characterized by:

$$\nabla \cdot (\sigma(\mathbf{x})\nabla v(\mathbf{x})) = -\nabla \cdot (\sigma(\mathbf{x})\nabla w(\mathbf{x})), \quad \mathbf{x} \in \Omega \quad (5)$$

$$v(\mathbf{x}) = 0, \quad \mathbf{x} \in \Gamma_D \quad (6)$$

$$\vec{n} \cdot \sigma(\mathbf{x})\nabla v(\mathbf{x}) = 0, \quad \mathbf{x} \in \Gamma_N \quad (7)$$

Here, one first projects the source term from the epicardium onto the function space over the entire domain (by setting w), then solves a homogeneous problem whose forcing function is the source after projection. This formulation reveals three approximation issues: 1) the accuracy of the epicardial potential $u_0(\mathbf{x})$, 2) the accuracy of the projection operator w , and 3) the accuracy of solving the homogeneous problem $v(\mathbf{x})$.

A practical finite element application tessellates Ω and constructs a set of basis functions $\{\phi_i\}$, each of which is associated with one node. The potential field $u(\mathbf{x})$ is approximated by the linear combination of the basis functions.

Wang, Kirby and Johnson are with the Scientific Computing and Imaging Institute, University of Utah. Email: {dfwang,kirby,crj}@sci.utah.edu. This work was funded by NSF Career Award (Kirby) NSF-CCF0347791 and NIH NCRR Grant No. 5P41RR012553-10.

The coefficient of each basis function is the potential value at its associated node. Substituting this expansion into (1) and applying the Galerkin method yield a linear system of the form:

$$\begin{pmatrix} \mathbf{A}_{II} & \mathbf{A}_{IT} \\ \mathbf{A}_{TI} & \mathbf{A}_{TT} \end{pmatrix} \begin{pmatrix} \mathbf{u}_I \\ \mathbf{u}_T \end{pmatrix} = \begin{pmatrix} -\mathbf{A}_{IH} \\ 0 \end{pmatrix} \mathbf{u}_H \quad (8)$$

where \mathbf{u}_H , \mathbf{u}_T , and \mathbf{u}_I denote the vector of potentials on the discretized heart surface (H), torso surface (T), and interior volume (I). The stiffness matrix A is given by $A_{i,j} = \int_{\Omega} \nabla \phi_i \nabla \phi_j$. A is partitioned based on the three divisions H, I , and T . Its capitalized subscript in (8) shows the interaction between each two divisions.

From (8) we derive the relation between \mathbf{u}_H and \mathbf{u}_T :

$$\mathbf{u}_T = \mathbf{K} \mathbf{u}_H \quad (9)$$

where \mathbf{K} is named the transfer matrix and severely ill-conditioned. The inverse ECG problem attempts to solve (9). Note that (8) is a special case of the general approach given by (5): the projection w is set piecewise-linear in the first layer of elements adjacent to the heart surface and zero elsewhere. (8) therefore exemplifies the aforementioned three issues. Once \mathbf{u}_H determines the resolution of the epicardial potentials, the accuracy of the FEM approximation is dictated by the discretization of the heart/volume projection (A_{IH}) and the volume conductor (the left-side matrix).

B. Inadequacy of Uniform Refinement for Inverse ECG

Most adaptive refinement strategies designed for forward problems are essentially equivalent to uniform refinement if not considering cost and efficiency. Although uniform refinement indeed improves the three approximation issues aforementioned, it worsens the conditioning property of K . Fig 1 compares the forward solution error and the singular values of K resulting from uniformly refining a 2D torso mesh. Singular value decomposition is an effective means for evaluating the numerical quality of K , because it constructs a spatial frequency spectrum for u_H and reveals how each frequency component contributes to the measurement u_T [2]. Evidently, a well-conditioned system is characterized by a slowly-descending singular value spectrum and a large proportion of nontrivial singular values.

Fig 1 shows that while uniform refinement reduces error in the forward problem, it simply extends the number of trivial singular values of K , thereby lowering the proportion of the recoverable components of u_H , which are associated with non-trivial singular values. This is because the ill-conditioning of K is an exponential function of the spatial frequency determined by the fidelity of epicardium [3]. Practitioners should assess this fidelity based on satisfying the clinical needs, but be cautious to solve beyond the limit. While the epicardium discretization gives the band-limit of the inverse solution one seeks to recover, the volume discretization determines the band-limit actually solvable.

For inverse problems, the aforementioned approximation principles should be stated as follows: (1) determine a reasonable resolution on epicardium and (2) refine the volume

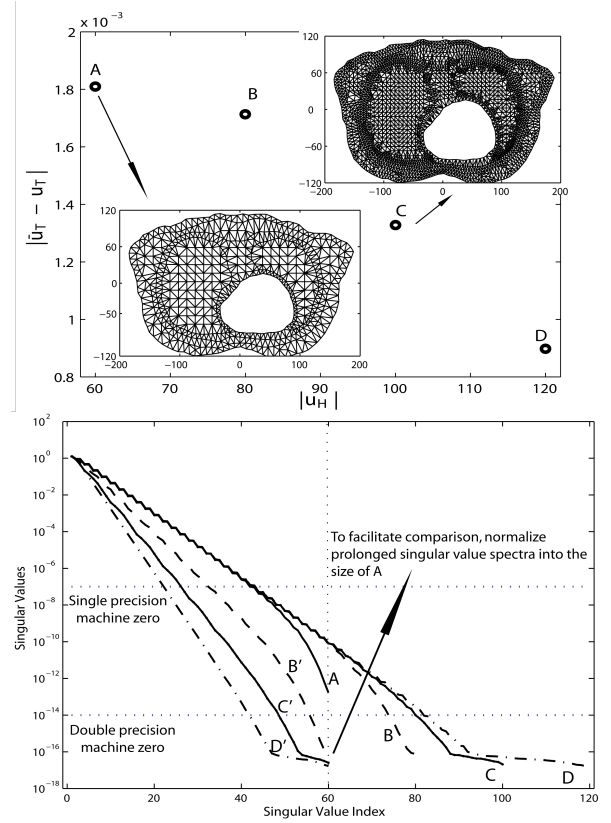


Fig. 1. (Top): forward solution error convergence with four increasingly refined meshes labeled as A-D. Only Mesh A and C are displayed. $|u_H|$ is the epicardial resolution, $|\bar{u}_T - u_T|$ means the forward solution error. (Bottom): singular value spectra of the resulting transfer matrix \mathbf{K} . Curves A-D are singular values in their original length; Curves B'-D' are normalized to the length of A, shown as B'-D'.

and heart/volume projection while fixing the heart boundary. Such requirement leads to our advocacy of hybrid finite elements and linear truncation from high-order finite elements.

C. Hybrid Finite Elements

The discretization of the inverse problem requires increasing the resolution normal to the epicardium while keeping the resolution on the epicardium. For triangular or tetrahedral elements, which are typically available in commodity mesh generators, such requirement leads to ill-shaped elements that by themselves cause extra numerical challenges. We place quadrilateral elements (2D) and prismatic elements (3D) around the epicardium, as illustrated by Fig 2. The quads/prisms can be refined along their normal direction to capture the high potential gradient near the heart, without affecting the resolution on the epicardium. Hybrid elements is simple to implement: we first built quads/prisms from the triangulated bounding surfaces before calling tetrahedral mesh-generating routines. This paper will present some results in 3D. We refer to [3] for detailed investigation of hybrid elements in 2D.

D. Linear Truncation from High-Order Elements

The finite element community has long been approximating continuous equations with high-order basis polynomials,

which achieve higher accuracy and faster convergence rate than linear finite elements. High-order interpolation in an element can be made hierarchical, composed by linear, quadratic, cubic basis functions, *etc.* The coefficients of linear components have a physical meaning of being the electrical potential value on the nodes of the element, whereas all high-order components are made zero on mesh nodes. It can be seen that a high-order FEM is built from a linear FEM, but adding approximation by higher-order polynomials. Accordingly, (9) can be rewritten as follows (for simplicity, we present a quadratic expansion here):

$$\begin{pmatrix} \mathbf{u}_T^1 \\ \mathbf{u}_T^2 \end{pmatrix} = \begin{pmatrix} K_{T,H}^{1,1} & K_{T,H}^{1,2} \\ K_{T,H}^{2,1} & K_{T,H}^{2,2} \end{pmatrix} \begin{pmatrix} \mathbf{u}_H^1 \\ \mathbf{u}_H^2 \end{pmatrix} \quad (10)$$

where the superscript indicates the order of each component of \mathbf{u}_T or \mathbf{u}_H . Our truncation scheme solves only the linear part of this high-order expansion:

$$\mathbf{u}_T^1 = K_{T,H}^{1,1} \mathbf{u}_H^1. \quad (11)$$

Such truncation is based on two concerns: (1) to preserve the pre-determined epicardium resolution, (2) \mathbf{u}_T is piecewise linear because measurements are made only on mesh nodes. Note that (11) differs from (9) in that it contains high-order expansion of A_{II} and A_{IH} given in (8).

This truncation scheme provides a seamless approach of refining the heart/torso projection and the volume conductor (by high-order FEM) while preserving the epicardial resolution (by truncation). As the truncation is conducted in a hierarchical polynomial space, it keeps the smoothness of the solution and avoids aspect-ratio problems that obstruct spatial refinement methods. Our experiments indicated third-order FEM was sufficient for the inverse ECG problem.

E. Regularization Methods

We solve the inverse problem (9) or (11) by the Tikhonov method applying both the 0-order and 1st-order constraints:

$$\mathbf{u}_H(\lambda) = \underset{\mathbf{u}_H}{\operatorname{argmin}} \{ \|\mathbf{K}\mathbf{u}_H - \mathbf{u}_T\|^2 + \lambda^2 (\|\mathbf{u}_H\|^2 + \alpha^2 \|\nabla \mathbf{u}_H\|^2) \} \quad (12)$$

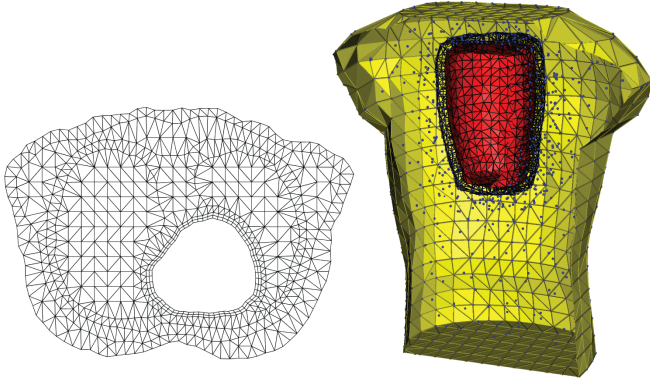


Fig. 2. (Left): a segmented 2D torso slice with two layers of quadrilaterals around the heart. (Right): the torso/cage geometry with one layer of prisms around the cage. The rest torso volume is filled by tetrahedra. For simplicity, volume mesh is not shown completely. The dark dots represent vertices of the tetrahedral volume mesh.

where $\|\cdot\|$ is the Euclidean norm. The values of λ and α are determined by exhaustive search. Our goal is to compare inverse solutions resulting from various refinements under an identical regularization framework.

III. RESULTS AND DISCUSSIONS

A. Hybrid Finite Elements

We present a hybrid elements model consisting of an isotropic torso tank and a canine heart surrounded by a cylinder cage on which potentials are measured. The model is illustrated by Fig 2. Using cage potentials rather than real epicardial potentials eliminates geometric variation incurred by heart contraction. The torso surface consists of 771 nodes and 1538 triangular elements whereas the cage has 602 nodes and 1200 triangles. This boundary discretization was kept intact during this test. We ran the forward simulation to obtain torso potentials, which, after being added with noise, served as the input for the inverse calculation. Fig 3 compares an ordinary tetrahedral mesh with a hybrid-element mesh having one layer of 10mm-thick prisms around the cage. The comparison is made in a coarse level and a refined level.

Fig 3 (top) shows that the hybrid mesh yields better singular values of \mathbf{K} than does the pure tetrahedral mesh under both discretization levels. The hybrid mesh achieves this numerical superiority with less elements, implying its advantage in efficiency. It can be seen that refining volume while keeping boundary resolutions extends non-trivial singular values of \mathbf{K} . This holds for both mesh types. In the tetrahedral meshes or hybrid meshes, the gap between the singular value spectrum of the coarse mesh and the spectrum of the refined mesh indicates the increased ill-conditioning caused by insufficient discretization but not associated with ill-posedness of the continuum problem. Any finite element discretization should consciously avoid such numerically-induced ill-conditioning.

Fig 3 (bottom) shows the cage potentials calculated under 1% input noise. The displayed potential map describes the instant when it had the largest spatial variances (thus the most difficult to recover). The current activation wavefront is captured well, although Tikhonov regularization tends to over-smooth the inverse solution. Hybrid meshes outperform pure tetrahedral meshes in recovering the magnitude of local extrema. Volume refinement leads to better recovery of the secondary local extrema (Panel C and D).

B. Linear Truncation from High-Order FEM

Our truncation method was conducted on a 2D torso mesh analogous to the one shown in Fig 2 but without quadrilaterals. The mesh, segmented to conform to interfaces between various tissues, contains 1071 triangles, including 60 nodes on the epicardium and 105 nodes on the torso surface. We tested isoparametric finite elements of first-, second-, and third-order, and the results are summarized in Fig 4. Fig 4(A) shows high-order refinement consistently improves the singular values of \mathbf{K} , a similar effect to spatial refinement of the volume. The convergence of singular values from the second-order FEM to the third-order FEM implies

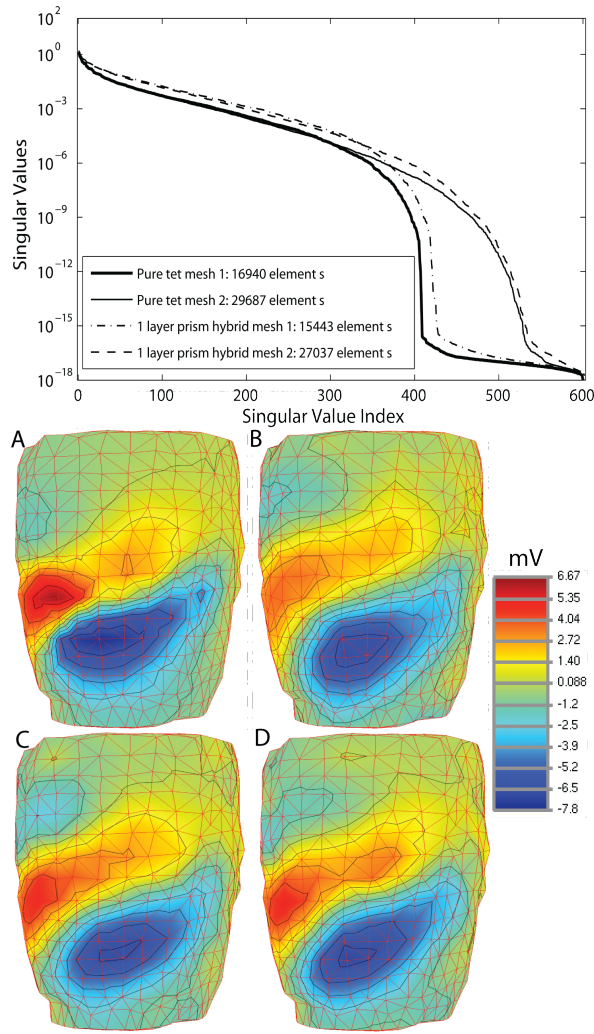


Fig. 3. (Top): singular values of \mathbf{K} resulting from pure tetrahedral meshes and hybrid meshes with one layer of prisms around the cage. Each mesh type includes two meshes that share identical boundary discretization but have different volume discretizations. (Bottom): cage potentials calculated from different meshes. (A) exact cage potentials; (B) potentials computed from pure tetrahedral mesh with 16940 elements; (C) potentials computed from hybrid mesh with coarse volume (15443 elements); and (D) potentials computed from hybrid mesh with refined volume (27037 elements).

the discretized problem has reached the same quality as the original continuous problem. In other words, refinement “saturates” to its asymptotic performance.

Fig 4(B) assesses the inverse solution by its relative error (the ratio of the error to the exact solution, in Euclidean norm) and its correlation coefficient with the exact solution. The inverse solution was calculated with zero-mean Gaussian noise of 30dB and 20dB being added to the torso measurements. With the truncation method, high-order refinement reduces the error from 8.3% to 6.7% under 30dB noise and from 17.5% to 9.7% under 20dB noise. It improves the correlation coefficient accordingly. Fig 4(C) demonstrates an example of reconstructed epicardial potentials under 20dB noise. It can be seen the linear truncation from third-order FEM yields the closest solution to the exact solution.

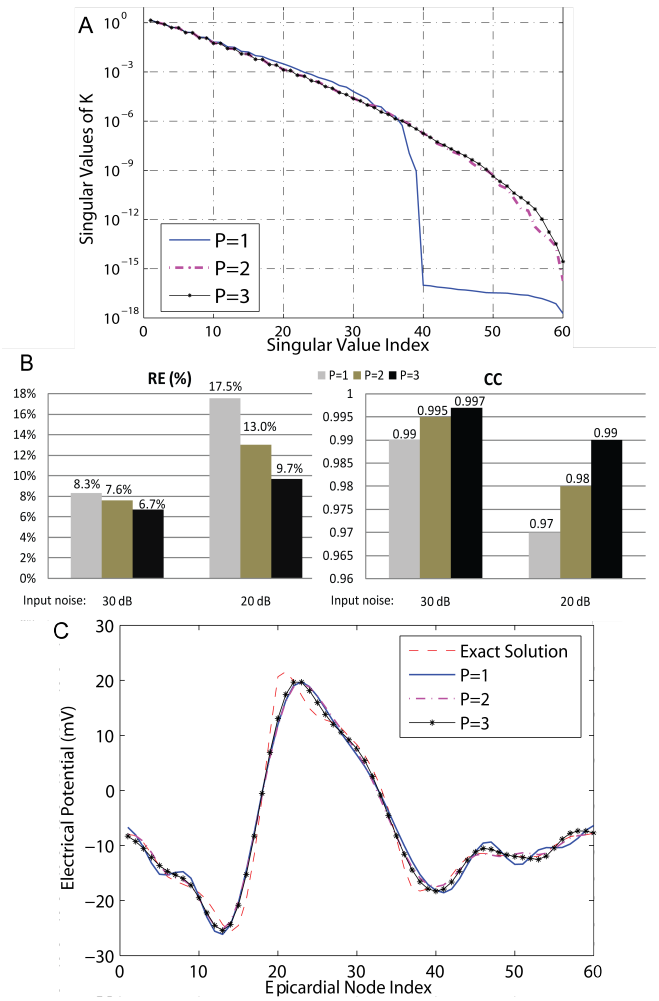


Fig. 4. Linear truncation from first-, second- and third-order finite elements, marked by $P = 1, 2, 3$. (A) singular values of the respective resulting \mathbf{K} ; (B) relative error (RE) and correlation coefficient (CC) of the inverse solution calculated under two levels of input noise; (C) reconstructed epicardial potentials under 20dB input noise.

IV. CONCLUSIONS

This paper explores the finite element refinement strategies for the inverse ECG problem. The strategies include preserving boundary resolution, refining the volume conductor and capturing the high potential gradient near the heart. To satisfy such requirements we propose hybrid-shaped finite elements and truncating linear components from high-order finite elements. Both methods effectively alleviate the ill-conditioning and improve the inverse solution.

REFERENCES

- [1] C. Johnson, “Adaptive finite element and local regularization methods for the inverse ECG problem,” in *Inverse Problems in Electrocardiology*, ser. Advances in Computational Biomedicine. WIT Press, 2001.
- [2] B. Messnarz, M. Seger, R. Modre, G. Fischer, F. Hanser, and B. Tilg, “A comparison of noninvasive reconstruction of epicardial versus transmbrane potentials in consideration of the null space,” *IEEE Trans Biomed Eng.*, vol. 51, no. 9, pp. 1609–1618, 2004.
- [3] D.Wang, R.M.Kirby, and C.R.Johnson, “Resolution strategies for the finite element based solution of the electrocardiograph inverse problem,” *accepted by IEEE Trans. Biomed. Eng.*, 2009, to appear.